Active-Power Control of Individual Converter Cells for a Battery Energy Storage System Based on a Multilevel Cascade PWM Converter

Laxman Maharjan, *Member, IEEE*, Tsukasa Yamagishi, and Hirofumi Akagi, *Fellow, IEEE*

***Abstract*—The battery energy storage system is an essential enabling device of the smart grid, because it helps grid connection of massive renewable energy resources. This paper has a brief discussion on a battery energy storage system based on a multilevel cascade pulsewidth-modulated (PWM) converter for its practical use. The active-power control of individual converter cells is presented to make it possible to charge and discharge the battery units at different power levels while producing a three-phase balanced line-to-line voltage. This results in the maximum utilization of battery energy even when the power-handling capabilities of the battery units differ. Experimental results obtained from a 200-V, 10-kW, 3.6-kWh battery energy storage system verify the effectiveness of the presented active-power control.**

***Index Terms*—Active-power control, battery energy storage systems, multilevel cascade converters, neutral shift.**

I. Introduction

MASSIVE penetration of renewable energy resources such as wind power and solar power is one of the major drivers of the smart grid in Japan. However, the renewable energy resources are intermittent in nature under the influence of meteorological fluctuations, which may produce a bad effect on grid voltage and frequency stabilization. Battery energy storage systems are indispensable to promote grid connections of massive renewable energy resources, thus making battery energy storage systems crucial in the smart grid.

Table I shows some major battery energy storage systems that have already been installed in the world [1]–[7]. The details for each system include the location, capacity, battery, application, and year of installation. The BEWAG AG's 17-MW 14-MWh system in Berlin, Germany, is the world's first large commercial battery energy storage system. Today, the 40-MW 14-MWh system in Golden Valley, Alaska, USA, and the 8-MW 58-MWh system in Hitachi Factory, Japan are the world's largest battery energy storage systems in terms of power and energy, respectively.

Traditional battery energy storage systems are based on combination of a multipulse (12-, 18-, 24-pulse, and so on) converter with a complicated zigzag transformer [3], [5]. The line-frequency transformer is expensive, bulky, lossy, and prone to failure. The lead-acid battery representing an established and mature technology has been preferable in the traditional systems. However, it has some serious drawbacks, including slow charging time, low energy density, end-of-life environmental concern, and short cycle life.

Modern battery energy storage systems are based on the combination of a multilevel converter such as diode clamped and cascade H-bridge topologies with an advanced battery technology, such as lithium (Li)-ion, sodium sulphur (NaS), nickel metal hydride (NiMH), and so on. ABB and Saft have recently developed a 600-kW, 200-kWh battery energy storage system based on a neutral-point clamped (NPC) converter and a Li-ion battery for the 11-kV distribution system of EDF Energy Networks, U.K. [8].

The multilevel cascade converter [9]–[14] may be one of the most suitable multilevel topologies for the modern battery energy storage systems. The authors of this paper discussed a battery energy storage system based on the combination of a multilevel cascade PWM converter with multiple NiMH battery units and addressed two key considerations for practical use [15], [16]. Reference [15] described the state-of-charge (SOC) balancing of the multiple battery units for effective utilization of battery energy, while [16] presented fault tolerance of the cascade converter for enhancing reliability and availability. There are, however, several other issues to be addressed as will be briefly explained in the following section. One of them is the active-power control of individual converter cells.

Manufacturing tolerances and operating conditions may cause small differences among multiple battery units in the multilevel cascade converter. These differences tend to be magnified over time, thus requiring individual power-handling capability to the battery units. This capability may also be required when one or more of the battery units in the cascade converter are replaced by new ones. For the maximum utilization of battery energy, it would then be necessary to operate one or more battery units at reduced or increased power levels.

Manuscript received February 15, 2010; revised May 15, 2010; accepted July 4, 2010. Date of current version February 7, 2012. Recommended for publication by Associate Editor P. Barbosa.

L. Maharjan was with the Department of Electrical and Electronic Engineering, Tokyo Institute of Technology, Meguro-ku 152-8552, Japan. He is now with Fuji Electric Europe GmbH, D-63067 Offenbach am Main, Germany (e-mail: maharjan@ieee.org).

T. Yamagishi was with the Department of Electrical and Electronic Engineering, Tokyo Institute of Technology, Meguro-ku 152-8552, Japan. He is now with Mitsubishi Heavy Industries Ltd., Komaki 485-8561, Japan (e-mail: tsukasa_yamagishi@mhi.co.jp).

H. Akagi is with the Department of Electrical and Electronic Engineering, Tokyo Institute of Technology, Meguro-ku 152-8552, Japan (e-mail: akagi@ee.titech.ac.jp).

Color versions of one or more of the figures in this paper are available online at http://ieeexplore.ieee.org.

Digital Object Identifier 10.1109/TPEL.2010.2059045

TABLE I
MAJOR BATTERY ENERGY STORAGE SYSTEMS INSTALLED IN THE WORLD

Battery Energy Storage System	Location	Capacity	Battery	Application	Year
BEWAG AG [1]	Berlin, Germany	17 MW/14 MWh	Lead acid	Spinning reserve, frequency control	1986
Kansai Electric Power Co., Inc. [2]	Tatsumi, Japan	1 MW/4 MWh	Lead acid	Multipurpose demonstration	1986
South California Edison (SCE) [3]	Chino, CA, USA	10 MW/40 MWh	Lead acid	Multipurpose demonstration	1988
Puerto Rico Electric Power Authority (PREPA) [4]	San Juan, PR, USA	20 MW/14 MWh	Lead acid	Spinning reserve, frequency control, voltage regulation	1994
GNB Technologies [5]	Vernon, CA, USA	5 MVA/2.5 MWh	Lead acid	Uninterruptible power supply (UPS), peak shaving	1995
Golden Valley Electric Association (GVEA) [6]	AK, USA	40 MW/14 MWh	Nickel cadmium (NiCd)	Spinning reserve, frequency control, voltage regulation	2003
Tokyo Electric Power Co., Inc. (TEPCO) [7]	Hitachi Factory, Japan	8 MW/58 MWh	Sodium sulphur (NaS)	Load leveling	2004

This paper presents the active-power control of individual converter cells for a battery energy storage system based on a multilevel cascade PWM converter. This control based on neutral shift[1] enables the multiple battery units to operate at different power levels while producing a three-phase balanced line-to-line voltage. Experimental results obtained from a 200-V, 10-kW, 3.6-kWh laboratory system verify the effectiveness of the control method.

II. CONSIDERATIONS ON THE BATTERY ENERGY STORAGE SYSTEM

Considerations on the battery energy storage system based on a multilevel cascade PWM converter can be categorized as follows:

1) SOC-balancing of battery units: Due to battery-unit tolerances, unequal converter-cell losses, and so on, SOC imbalance may occur among multiple battery units. This may result in reducing the total availability of the battery units and may also cause overcharge/overdischarge of a particular battery unit. An SOC-balancing control is, therefore, indispensable. Tolbert *et al*. [17] described a switching-pattern-swapping method for SOC balancing in a multilevel cascade converter with staircase modulation for a motor drive. The authors of this paper presented SOC balancing in a multilevel cascade converter with pulsewidth modulation for a battery energy storage system [15].

2) Fault tolerance: The cascade-converter-based battery energy storage system employs a large number of power switching devices, which increases the chances of failure. Fault tolerance is desirable to maintain continuous operation during a converter-cell or battery-unit failure, thus improving the reliability and availability of the system.

Wei *et al*. [18], and Rodriguez *et al*. [19] described fault-tolerant controls for cascade-converter-based motor drives combining converter-cell bypass with neutral shift. Song and Huang [20] achieved fault tolerance in a cascade-converter-based STATCOM, placing a redundant converter cell in each phase and bypassing not only the faulty converter cell but also two healthy converter cells in the other two phases. The authors of this paper presented a fault-tolerant control based on neutral shift for a battery energy storage system, which can produce a three-phase balanced line-to-line voltage and achieve SOC balancing of the other healthy battery units during a converter-cell failure [16].

3) Active-power control of individual converter cells: Production tolerances, uneven temperature conditions, and differences in ageing characteristics may eventually bring one or more battery units to reduced power-handling capacities. Therefore, an active-power control of individual converter cells is indispensable to enable the multiple battery units operate at different power levels. It is also advantageous when one or more of the battery units are replaced by new ones. This paper discusses the issue in detail.

4) Ride-through capability of asymmetrical power system faults: The fault-tolerant controls described in [16], [18]–[20] dealt with internal faults. However, when the battery energy storage system is connected to a power distribution system, it has to withstand asymmetrical power system failures such as single-line-to-ground (SLG) faults. Ride-through capability of such faults is desirable. The multilevel cascade PWM converter for a battery energy storage system can actively produce an amount of negative-sequence voltage in response to system voltage imbalance, thereby suppressing the negative-sequence current resulting from the system voltage imbalance.

5) Startup method: A simple startup method without using external circuit is important. This paper describes such a procedure for the battery energy storage system based on the method presented in [21] for a cascade-converter-based STATCOM.

6) Cell balancing: Cell balancing is a method of saving weaker cells by adjusting an appropriate amount of charging and discharging on the cells in each battery unit. It is essential for extending battery life and has been investigated in many literatures [22], [23].

[1]Neutral shift means shifting the neutral point of the floating (ungrounded) neutral point of the star-configured cascade converter away from the neutral point of the source or the ac mains.

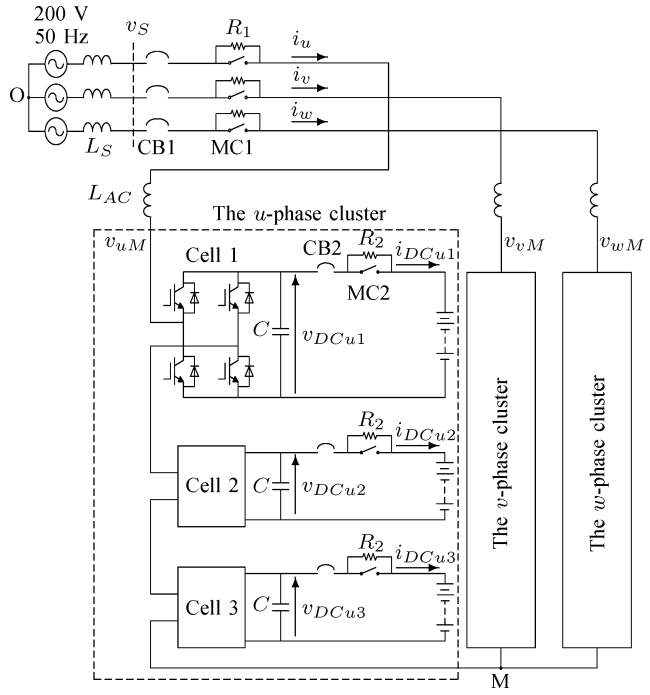

Fig. 1. Experimental system configuration of the 200-V, 10-kW, 3.6-kWh downscaled energy storage system based on combination of a three-phase cascade PWM converter with a cascade number $N = 3$ and nine NiMH battery units with a nominal voltage of 72 V.

7) Optimization between the cascade number and the dc voltage: The cascade number[2] affects communication and reliability issues while the dc voltage affects cost and life issues of battery units. Therefore, optimization between them is an important design consideration.

8) Battery cost and life: The cost and life of battery units are the major hurdles in putting large-scale battery energy storage systems into practical use. Comprehensive research and development have to be achieved on cost reduction and life expansion.

III. The 200-V, 10-kW, 3.6-kWh Experimental Battery Energy Storage System

Fig. 1 shows the system configuration of the 200-V, 10-kW, 3.6-kWh experimental battery energy storage system based on a multilevel cascade PWM converter. Table II summarizes the circuit parameters. The star-configured system has a cascade number $N = 3$.

Each of the nine H-bridge converter cells has a 72-V 5.5-Ah nickel-metal-hybride (NiMH) battery unit connected at its dc link. Each battery unit is equipped with a battery management system (BMS) that provides the functions of monitoring and controlling the respective battery unit to protect it against abnormal operation.

Fig. 2 shows the control system of the 200-V system. This is based on a fully digital controller, using a DSP and multiple field-programmable gate arrays (FPGAs). The nine converter cells are controlled by phase-shifted unipolar sinusoidal PWM with a carrier frequency of 800 Hz [21], [24]. The resulting line-to-neutral voltage is a seven-level waveform with an equivalent carrier frequency of 4.8 kHz.

[2]The term "cascade number" implies the number of cascaded converter cells in a phase.

TABLE II
Circuit Parameters of the Experimental Battery Energy Storage System

Nominal line-to-line rms voltage	V_S	200 V
Power rating	P	10 kW
Cascade number	N	3
AC inductor	L_{AC}	1.2 mH (10%)
Background system inductance	L_S	48 μH (0.4%)
Starting resistors	$R_1,\ R_2$	10 Ω, 20 Ω
Nominal DC voltage	V_{DC}	72 V
DC capacitor	C	16.4 mF
Unit capacitance constant	H	38 ms at 72 V
NiMH battery unit		72 V, 5.5 Ah × 9
PWM carrier frequency		800 Hz
Equivalent carrier frequency		4.8 kHz

on a three-phase, 200-V, 10-kW, 50-Hz base.

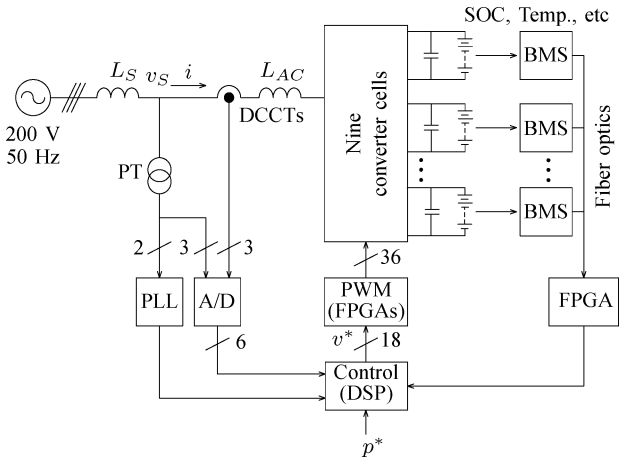

Fig. 2. Control system for the battery energy storage system.

IV. Active-Power Control of Individual Converter Cells

Fig. 3 shows the block diagram of active-power control for the battery energy storage system. The active-power control consists of two parts:

1) active-power control of the whole converter cells (represented by dashed lines) and
2) active-power control of individual converter cells (represented by solid lines).

The first one based on the synchronous dq reference frames has the responsibility of the total active-power control. The authors have already described it in detail in [25], where the modulating signals v^*_{uO}, v^*_{vO}, and v^*_{wO} are obtained by applying the inverse dq transformation to the following equation:

$$\begin{bmatrix} v_d^* \\ v_q^* \end{bmatrix} = \begin{bmatrix} v_{Sd} \\ v_{Sq} \end{bmatrix} - \begin{bmatrix} 0 & -\omega L_{AC} \\ \omega L_{AC} & 0 \end{bmatrix} \begin{bmatrix} i_d \\ i_q \end{bmatrix} - K \begin{bmatrix} i_d^* - i_d \\ i_q^* - i_q \end{bmatrix} - \frac{K}{T} \int \begin{bmatrix} i_d^* - i_d \\ i_q^* - i_q \end{bmatrix} dt. \quad (1)$$

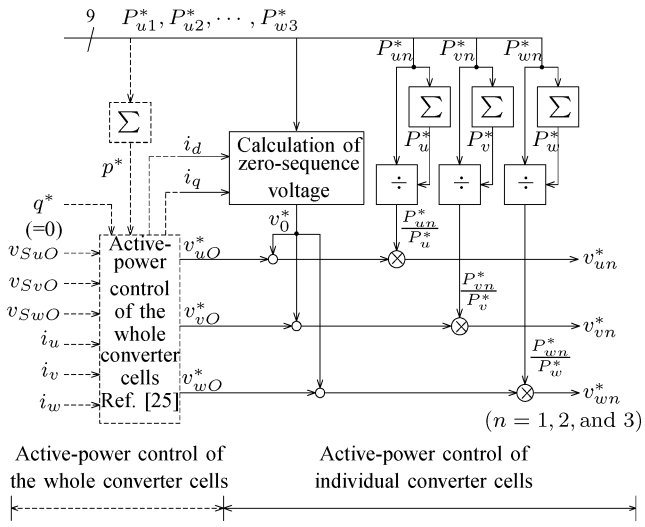

Fig. 3. Block diagram of the active-power control of the battery energy storage system consisting of two parts. The part represented by solid lines is the active-power control of individual converter cells, while that represented by dashed lines is the active-power control of the whole converter cells.

Here, v_{Sd} and v_{Sq} are the d-axis and q-axis components of $\vec{v}$, while i_d and i_q are those of $\vec{i}$. The d-axis current command i^*_d and the q-axis current command i^*_q are given by

$$i^*_d = \frac{p^*}{v_{Sd}} \tag{2}$$

$$i^*_q = \frac{q^*}{v_{Sd}} = 0 \tag{3}$$

where p^* is the total active power command, while the reactive power command of $q^* = 0$ ensures unity power factor operation. Note that the first term on the right-hand side of (1) is a voltage feedforward control, while the third and fourth terms form a current feedback control.

The active-power control of the whole converter cells works under the assumption that all the battery units have the same power-handling capabilities. This is, however, not always true as is explained in Section I. Therefore, the active-power control of individual converter cells is introduced, which is based on modifying the output signals from the active-power control of the whole converter cells is such a way that the actual converter-cell powers P_{un}, P_{vn}, and P_{wn} follow their references with different power levels. Its main function is to calculate the amplitude $\sqrt{2}\,V_0$ and phase angle ϕ_0 of the zero-sequence voltage v^*_0 to be injected in such a way as to produce a three-phase balanced line-to-line voltage, even when the nine converter cells are operated at different power levels. The following is the detailed analysis of the active-power control of individual converter cells.

If the cascade converter voltage is assumed not to contain any negative-sequence voltage, it can be expressed as

$$\begin{bmatrix} \dot{V}_{uM} \\ \dot{V}_{vM} \\ \dot{V}_{wM} \end{bmatrix} = \begin{bmatrix} \dot{V}_{fuM} \\ \dot{V}_{fvM} \\ \dot{V}_{fwM} \end{bmatrix} + \begin{bmatrix} \dot{V}_0 \\ \dot{V}_0 \\ \dot{V}_0 \end{bmatrix} = V_{fM}\, e^{j\phi_f} \begin{bmatrix} 1 \\ e^{-j\frac{2\pi}{3}} \\ e^{j\frac{2\pi}{3}} \end{bmatrix} + V_0 e^{j\phi_0} \begin{bmatrix} 1 \\ 1 \\ 1 \end{bmatrix} \tag{4}$$

where the first term on the right-hand side represents the positive-sequence voltage with an rms magnitude of V_{fM} and a phase angle of ϕ_f with respect to the u-phase voltage. The second term represents the fundamental-frequency zero-sequence voltage with an rms magnitude of V_0 and a phase angle of ϕ_0. Both V_0 and ϕ_0 are adjusted by the active-power control of individual converter cells.

The line currents are assumed to contain only the following positive-sequence currents.

$$\begin{bmatrix} \dot{I}_u \\ \dot{I}_v \\ \dot{I}_w \end{bmatrix} = I e^{j\delta} \begin{bmatrix} 1 \\ e^{-j\frac{2\pi}{3}} \\ e^{j\frac{2\pi}{3}} \end{bmatrix} \tag{5}$$

where

$$I = \sqrt{\frac{I_d^2 + I_q^2}{3}} \tag{6}$$

$$\delta = \begin{cases} \tan^{-1}\frac{I_q}{I_d}, & \text{if } I_d \neq 0 \\ \frac{\pi}{2}, & \text{if } I_d = 0 \text{ and } I_q > 0 \\ -\frac{\pi}{2}, & \text{if } I_d = 0 \text{ and } I_q < 0. \end{cases} \tag{7}$$

In a sinusoidal steady-state condition, I_d and I_q are equal to the d-axis current i_d and the q-axis current i_q. The u-phase power can be expressed as

$$P_u = \mathrm{Re}\left[\dot{V}_{uM} \cdot \bar{\dot{I}}_u\right] = \mathrm{Re}\left[\dot{V}_{fuM} \cdot \bar{\dot{I}}_u + \dot{V}_0 \cdot \bar{\dot{I}}_u\right]. \tag{8}$$

The first term on the right-hand side is the active power related to the positive-sequence voltage included in the u-phase ac voltage of the cascade converter, while the second term is the active power coming from the zero-sequence-voltage injection, which can be expressed as

$$\begin{aligned} P_{u0} &= \mathrm{Re}\left[\dot{V}_0 \cdot \bar{\dot{I}}_u\right] \\ &= \mathrm{Re}\left[(V_0(\cos\phi_0 + j\sin\phi_0) \cdot I(\cos\delta + j\sin\delta)\right] \\ &= V_0 I \cos(\phi_0 - \delta). \end{aligned} \tag{9}$$

Similarly, the v- and w-phase powers due to the zero-sequence voltage can be calculated.

$$\begin{bmatrix} P_{u0} \\ P_{v0} \\ P_{w0} \end{bmatrix} = V_0 I \begin{bmatrix} \cos(\phi_0 - \delta) \\ \cos\left(\phi_0 - \delta + \frac{2\pi}{3}\right) \\ \cos\left(\phi_0 - \delta - \frac{2\pi}{3}\right) \end{bmatrix}. \tag{10}$$

Let P^*_{un}, P^*_{vn}, and P^*_{wn} be the power commands to the $3N$ converter cells, where $n = 1, 2, \ldots N$. The three cluster power commands P^*_u, P^*_v, and P^*_w are given by

$$\begin{bmatrix} P^*_u \\ P^*_v \\ P^*_w \end{bmatrix} = \begin{bmatrix} P^*_{u1} + P^*_{u2} + \ldots + P^*_{uN} \\ P^*_{v1} + P^*_{v2} + \ldots + P^*_{vN} \\ P^*_{w1} + P^*_{w2} + \ldots + P^*_{wN} \end{bmatrix}. \tag{11}$$

Each of the cluster power commands can be considered as a sum of two components as follows:

$$\begin{bmatrix} P_u^* \\ P_v^* \\ P_w^* \end{bmatrix} = \frac{P^*}{3} + \begin{bmatrix} \Delta P_u^* \\ \Delta P_v^* \\ \Delta P_w^* \end{bmatrix}, \tag{12}$$

where $P^* = P_u^* + P_v^* + P_w^*$. The first term on the right-hand side of (12) is the active power due to the positive-sequence voltage. The second term is the active power due to the zero-sequence voltage. From (10), it is given by

$$\begin{bmatrix} \Delta P_u^* \\ \Delta P_v^* \\ \Delta P_w^* \end{bmatrix} = V_0 I \begin{bmatrix} \cos(\phi_0 - \delta) \\ \cos\left(\phi_0 - \delta + \dfrac{2\pi}{3}\right) \\ \cos\left(\phi_0 - \delta - \dfrac{2\pi}{3}\right) \end{bmatrix}. \tag{13}$$

Solving (13) for V_0 and ϕ_0 results in

$$\phi_0 - \delta = \begin{cases} \tan^{-1}\left[\dfrac{2}{\sqrt{3}}\left(\dfrac{1}{2} + \cdot\dfrac{\Delta P_v^*}{\Delta P_u^*}\right)\right] \text{ if } \Delta P_u^* \neq 0 \\ \dfrac{\pi}{2} \quad \text{if } \Delta P_u^* = 0 \text{ and } \Delta P_v^* > 0 \\ -\dfrac{\pi}{2} \quad \text{if } \Delta P_u^* = 0 \text{ and } \Delta P_v^* < 0 \end{cases} \tag{14}$$

$$V_0 = \frac{\Delta P_u^*}{I\cos(\phi_0 - \delta)}. \tag{15}$$

The zero-sequence-voltage reference is determined as

$$v_0^* = \sqrt{2}\, V_0\, \sin(\omega t + \phi_0). \tag{16}$$

Finally, the modulating signals to the $3N$ converter cells are determined as

$$v_{un}^* = (v_{uO}^* + v_0^*)\,\frac{P_{un}^*}{P_u^*} \tag{17}$$

$$v_{vn}^* = (v_{vO}^* + v_0^*)\,\frac{P_{vn}^*}{P_v^*} \tag{18}$$

$$v_{wn}^* = (v_{wO}^* + v_0^*)\,\frac{P_{wn}^*}{P_w^*}. \tag{19}$$

Note that when the power-handling capacities of all the $3N$ battery units are equal, their active power commands are also equal ($P_{un}^* = P_{vn}^* = P_{wn}^*$). Therefore, the modulating signals would be solely determined by the active-power control of the whole converter cells.

$$v_{un}^* = \frac{v_{uO}^*}{N} \tag{20}$$

$$v_{vn}^* = \frac{v_{vO}^*}{N} \tag{21}$$

$$v_{wn}^* = \frac{v_{wO}^*}{N}. \tag{22}$$

The active-power control of the individual converter cells is basically a feedforward control. However, a feedback loop, as shown in Fig. 4, is used in the experiment to make the $3N$ converter-cell powers at the dc side, P_{un}, P_{vn}, and P_{wn} equal to the respective commands at the ac side, P_{un}^*, P_{vn}^*, and P_{wn}^*, regardless of the converter-cell losses. The proportional gain

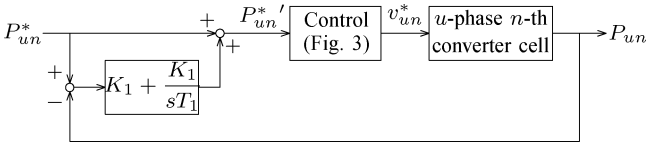

Fig. 4. Feedback loop (taking the u-phase as an example) used in the experiment to make the converter-cell powers at the dc side, P_{un} equal to the respective commands at the ac side, P_{un}^*, regardless of the converter-cell losses.

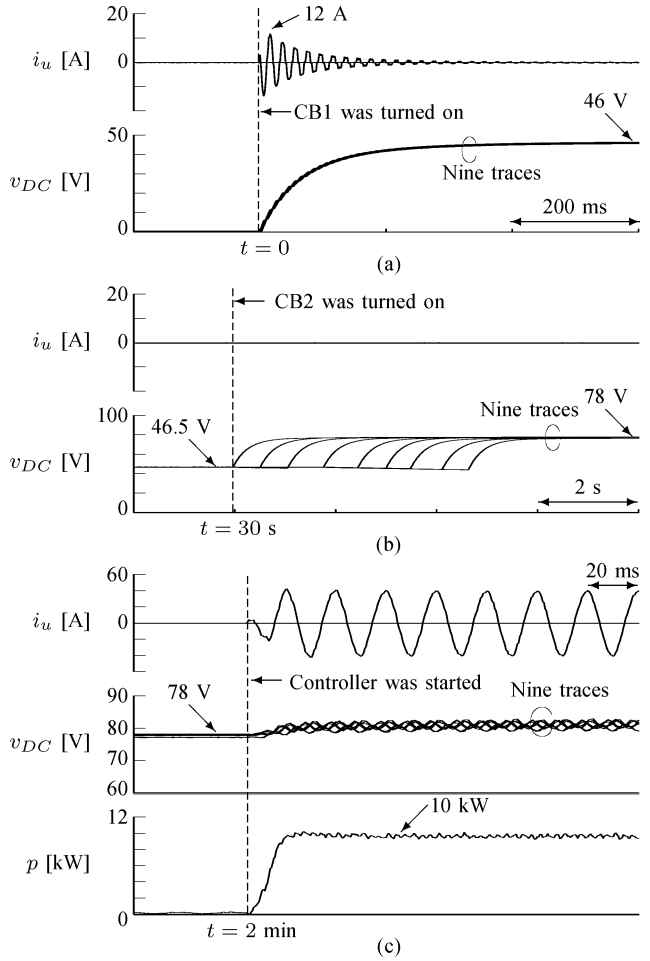

Fig. 5. Experimental waveforms when the battery energy storage system was started. (a) CB1 was turned on at $t = 0$. (b) CB2 was turned on at $t = 30$ s. (c) Controller was started at $t = 2$ min.

K_1 and the integral time constant T_1 of the PI controller in the feedback loop are set as follows:

$$K_1 = 0.1\text{W/W} \qquad T_1 = 10\text{ s}. \tag{23}$$

For simplicity, the feedback loop has been neglected from the earlier analysis.

V. Waveforms During Startup

The battery energy storage system requires no external startup circuit. Fig. 1 includes a simple startup circuit consisting of the following two subcircuits:

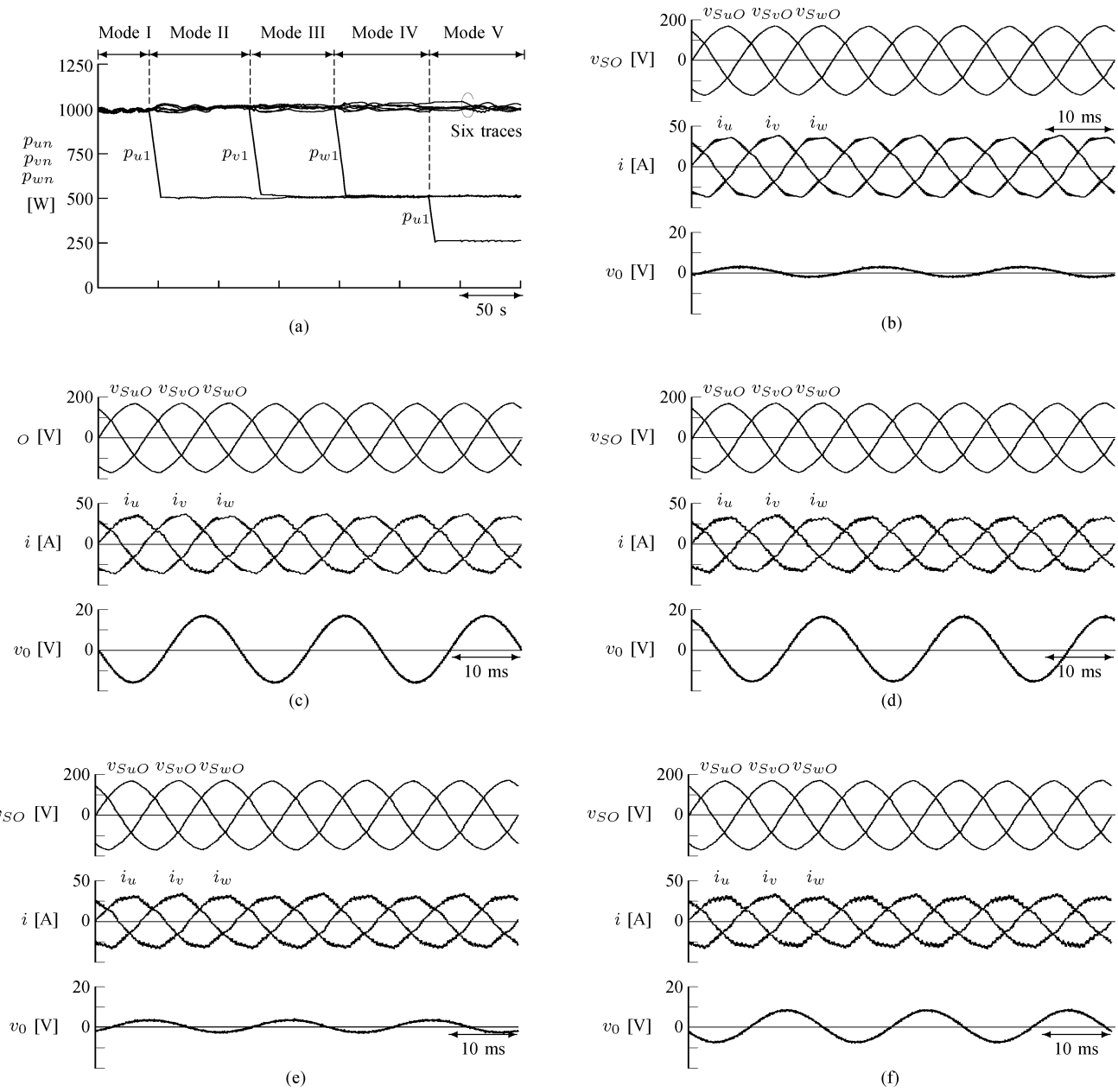

Fig. 6. Experimental waveforms during five modes of operation of Table III. (a) Power waveforms of the nine converter cells. (b) Mode I. (c) Mode II. (d) Mode III. (e) Mode IV. (f) Mode V.

1) the ac startup circuit consisting of the three-phase circuit breaker CB1, the three-phase magnetic contactor MC1, and the current-limiting resistor R_1 in each phase, and
2) the dc startup circuit consisting of the circuit breaker CB2, the magnetic contactor MC2, and the current limiting resistor R_2 in each converter cell.

Fig. 5 shows the waveforms during startup. At time $t = 0$, CB1 was switched on, whereas MC1 as well as CB2 and MC2 in each converter cell remained switched off. Each of the nine capacitors started charging through R_1, and the respective converter cell was operating as a diode rectifier. The inrush ac current was limited to 12 A (peak), which was below the rated current of 30 A. At the time of $t = 30$ s, when the starting ac current decayed to zero, the MC1 as well as nine CB2s were turned on sequentially. Then, the dc-link voltages reached the battery-unit voltages of 78 V, as shown in Fig. 5(b). The nine starting resistors R_2 limit the inrush dc currents when the nine battery units are connected to the dc links and are bypassed by the nine magnetic contactors MC2s in 5 s. At $t = 2$ min, the controller was started, and the gate signals were provided to the nine converter cells, along with the active power commands. The system thus came to normal operation.

VI. Experimental Verification of Active-Power Control of Individual Converter Cells

Table III summarizes five modes of operation of the experimental system. For each mode, it gives the nine converter-cell

TABLE III
FIVE MODES OF OPERATION, EACH OF WHICH HAS A DIFFERENT SET OF CONVERTER-CELL POWER COMMANDS, AND ITS CORRESPONDING ZERO-SEQUENCE VOLTAGE

Mode	Converter-cell power commands [kW]									Zero-sequence voltage v_0	
	P^*_{u1}	P^*_{u2}	P^*_{u3}	P^*_{v1}	P^*_{v2}	P^*_{v3}	P^*_{w1}	P^*_{w2}	P^*_{w3}	$\sqrt{2}V_0$ [V]	ϕ_0 [rad]
I	1	1	1	1	1	1	1	1	1	0	-
II	0.5	1	1	1	1	1	1	1	1	19.2	$-\pi$
III	0.5	1	1	0.5	1	1	1	1	1	20.4	$2\pi/3$
IV	0.5	1	1	0.5	1	1	0.5	1	1	0	-
V	0.25	1	1	0.5	1	1	0.5	1	1	11.3	$-\pi$

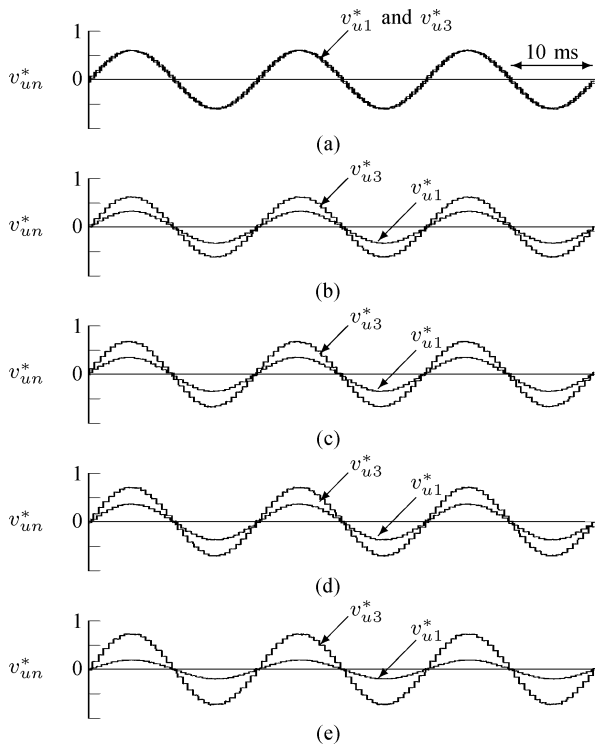

Fig. 7. Modulating signals (normalized by respective battery-unit voltages) of u-phase converter-cells numbered 1 and 3. (a) Mode I. (b) Mode II. (c) Mode III. (d) Mode IV. (e) Mode V.

power commands and shows the theoretical values of the amplitude and phase angle of the corresponding zero-sequence voltage v_0. The zero-sequence voltage is determined in such a way as to produce a three-phase balanced line-to-line voltage, even when the nine converter cells are operated at different power levels.

Fig. 6(a) shows experimental power waveforms of the nine converter cells for the five modes of operation in Table III. The nine powers were measured at the dc sides by the respective battery management systems. Mode I represents the condition when the power commands to all the nine converter cells were equal (1 kW each). From mode II to mode V, one of the nine converter-cell power commands was reduced to 50% of its previous value in a ramp of 50 W/s.

Fig. 6(b) shows experimental waveforms in mode I. With equal power commands to all the nine converter cells, the zero-sequence voltage should be theoretically zero as indicated in

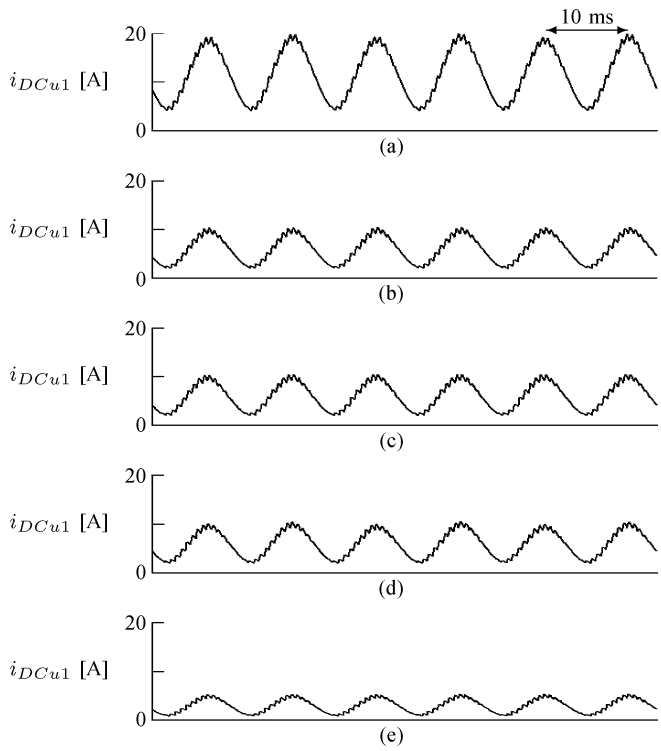

Fig. 8. Experimental waveforms of the battery current in the u-phase converter-cell numbered 1. (a) Mode I. (b) Mode II. (c) Mode III. (d) Mode IV. (e) Mode V.

Table III. However, due to the feedback loop of power in Fig. 4, a small amount of zero-sequence voltage was observed. The zero-sequence voltage with a peak of 2 V was in phase with the u-phase current. As a result, the u-cluster drew an additional power of 30 W. The total harmonic distortion (THD) of u-phase current i_u was 4.0%.

Fig. 6(c) shows the experimental waveforms in mode II. While the power command of the u-phase converter-cell numbered 1 was reduced to 0.5 kW, the zero-sequence voltage was 17 V in amplitude, and out of phase by 180° with respect to the u-phase voltage. A small difference between experimental and theoretical amplitudes was caused again by the power feedback loop. The current THD was 4.8% in this case due to an increased 1.6-kHz ripple.

Fig. 6(d) shows the experimental waveforms in mode III. The power command of the v-phase converter-cell numbered 1 was reduced to 0.5 kW, whereas those of the u-phase converter cell numbered 1 and other seven converter cells were kept at 0.5 and 1 kW, respectively. The injected zero-sequence voltage was 18 V in amplitude and in phase with the w-phase voltage. The current THD was 5% in this case.

Fig. 6(e) shows the experimental waveforms in mode IV. With equal power commands in the u-, v- and w-clusters (2.5 kW each), the resulting zero-sequence should theoretically be zero. A small amount of zero sequence voltage was, however, observed as in Mode I. The current THD was 4.6%.

Fig. 6(f) shows the experimental waveforms in mode V. The power command of the u-phase converter-cell numbered 1 was reduced to 0.25 kW, whereas those of the v- and w-phase

converter cells numbered 1 were kept at 0.5 kW, and those of the other six converter cells were kept at 1 kW. The resulting zero-sequence voltage was 9 V in amplitude, and out of phase by 180° with respect to the u-phase voltage. The current THD was 6%.

Since the same ac current flows through the three converter cells in a cluster, the desired sharing of power between the three converter cells in the cluster is achieved by proportionally controlling the ac voltages of the three converter cells. That means that, taking u-phase as an example, the following relation exists as indicated in (17):

$$\frac{Vu1}{P_{u1}} = \frac{V_{u2}}{P_{u2}} = \frac{V_{u3}}{P_{u3}}. \tag{24}$$

Fig. 7 shows the modulating signals (normalized by respective battery-unit voltages that were assumed equal) of the u-phase converter cells numbered 1 and 3 for the five modes of operation. The power command P^*_{u3} to the u-phase converter cell numbered 3 was kept constant at 1 kW throughout the five modes of operation. Then, the power command P^*_{u1} to the u-phase converter cell numbered 1 was changed from 1 to 0.5 kW in mode II, and again from 0.5 to 0.25 kW in mode V. As a result, the ratio of V^*_{u1} to V^*_{u3} was changed from 1 to 0.5 in mode II, and from 0.5 to 0.25 in mode V, as expected.

Fig. 8 shows the battery-unit current $i_{\mathrm{dc}u1}$ of the u-phase converter cell numbered 1 for the five modes of operation. The battery current contained the 100-Hz component as well as the 1.6-kHz component due to PWM.

VII. Conclusion

This paper has described a battery energy storage system based on a multilevel cascade PWM converter with star configuration from a practical point of view. The presented active-power control of individual converter cells enables the multiple battery units to operate at different power levels while producing a three-phase balanced line-to-line voltage. Experimental results based on a 200-V, 10-kW, 3.6-kWh system have verified the effectiveness of the presented active-power control.

References

[1] R. Saupe, "The power conditioning system for the ±8.5/17 MW energy storage plant of BEWAG," in *Proc. 3rd Int. Conf. Power Electron. Variable-Speed Drives*, Jul. 1988, pp. 218–220.

[2] T. Nakayama, Y. Sera, and A. Mitsuda, "The current status of development of advanced battery electric energy storage systems in Japan," in *Proc. 24th Intersoc. Energy Convers. Eng. Conf. (IECEC 1989)*, Aug., vol. 3, pp. 1297–1301.

[3] L. H. Walker, "10-MW GTO converter for battery peaking service," *IEEE Trans. Ind. Appl.*, vol. 26, no. 1, pp. 63–72, Jan./Feb. 1990.

[4] P. A. Taylor, "Update on the Puerto Rico electric power authority's spinning reserve battery system,"in *Proc. IEEE Battery Conf. Appl. Adv.*, Jan. 1996, pp. 249–252.

[5] N. W. Miller, R. S. Zrebiec, R. W. Delmerico, and G. Hunt, "Design and commissioning of a 5-MVA, 2.5-MWh battery energy storage," in *Proc. IEEE Transmiss. Distrib. Conf.*, Sep. 1996, pp. 339–345.

[6] T. DeVries, J. McDowall, N. Umbricht, and G. Linhofer, "Cold storage: The battery energy storage system for Golden Valley Electric Association," *ABB Rev.*, vol. 1/2004, pp. 38–43, 2004.

[7] J. Baker, "New technology and possible advances in energy storage," *Energy Policy*, vol. 36, no. 12, pp. 4368 –4373, Dec. 2008.

[8] N. Wade, P. Taylor, P. Lang, and J. Svensson, "Energy storage for power flow management and voltage control on an 11kV UK distribution network," in *Proc. CIRED 2009*, Jun., pp. 1–4.

[9] R. H. Baker and L. H. Bannister, "Electric power converter," U.S. Patent 3 867 643, Feb. 1975.

[10] M. Marchesoni, M. Mazzucchelli, and S. Tenconi, "A nonconventional power converter for plasma stabilization," *IEEE Trans. Power Electron.*, vol. 5, no. 2, pp. 212–219, Apr. 1990.

[11] F. Z. Peng, J. S. Lai, J. W. McKeever, and J. VanCoevering, "A multilevel voltage-source inverter with separate dc sources for static var generation," *IEEE Trans. Ind. Appl.*, vol. 32, no. 5, pp. 1130–1138, Sep./Oct. 1996.

[12] P. W. Hammond, "A new approach to enhance power quality for medium voltage ac drives," *IEEE Trans. Ind. Appl.*, vol. 33, no. 1, pp. 202–208, Jan./Feb. 1997.

[13] J. D. Ainsworth, M. Davies, P. J. Fitz, K. E. Owen, and D. R. Trainer, "Static var compensator (STATCOM) based on single phase chain circuit converters," *IEE Proc.—Gener. Transm. Distrib.*, vol. 145, no. 4, pp. 381–386, Jul. 1998.

[14] J. Rodriguez, S. Bernet, B. Wu, J. O. Pontt, and S. Kouro, "Multilevel voltage-source-converter topologies for industrial medium-voltage drives," *IEEE Trans. Ind. Electron.*, vol. 54, no. 6, pp. 2930–2945, Dec. 2007.

[15] L. Maharjan, S. Inoue, H. Akagi, and J. Asakura, "SOC (state-of-charge)-balancing control of a battery energy storage system based on a cascade PWM converter," *IEEE Trans. Power Electron.*, vol. 24, no. 6, pp. 1628–1636, Jun. 2009.

[16] L. Laxman, T. Yamagishi, H. Akagi, and J. Asakura, "Fault-tolerant control for a battery energy storage system based on a cascade PWM converter with star configuration" *IEEE Trans. Power Electron.*, vol. 25, no. 9, pp. 2386–2396, Sep. 2010.

[17] L. M. Tolbert, F. Z. Peng, and T. G. Habetler, "Multilevel converters for large electric drives," *IEEE Trans. Ind. Appl.*, vol. 35, no. 1, pp. 36–44, Jan./Feb. 1999.

[18] S. Wei, B. Wu, F. Li, and X. Sun, "Control method for cascaded H-brige multilevel inverter with faulty power cells," in *Proc. IEEE APEC*, Feb. 2003, vol. 1, pp. 261–267.

[19] J. Rodriguez, P. W. Hammond, J. Pontt, R. Musalem, P. Lezana, and M. J. Escobar, "Operation of a medium-voltage drive under faulty conditions," *IEEE Trans. Ind. Electron.*, vol. 52, no. 4, pp. 1080–1085, Aug. 2005.

[20] W. Song and A. Q. Huang, "Control strategy for fault-tolerant cascaded multilevel converter based STATCOM," in *Proc. IEEE APEC*, Feb./Mar. 2007, pp. 1073–1076.

[21] Y. Liang and C. O. Nwankpa, "A new type of STATCOM based on cascading voltage-source inverters with phase-shifted unipolar SPWM," *IEEE Trans. Ind. Appl.*, vol. 35, no. 5, pp. 1118–1123, Sep./Oct. 1999.

[22] N. H. Kutkut and D. M. Divan, "Dynamic equalization techniques for series battery stacks," in *Proc. IEEE INTELEC 1996*, Oct., pp. 514–521.

[23] S. W. Moore and P. J. Schneider, "A review of cell equalization methods for lithium ion and lithium polymer battery systems," in *Proc. SAE World Congress*, Mar. 2001, Doc. No 2001-01-0959.

[24] D. G. Holmes and B. P. McGrath, "Opportunities for harmonic cancellation with carrier-based PWM for two-level and multilevel cascaded inverters," *IEEE Trans. Ind. Appl.*, vol. 37, no. 2, pp. 574–582, Mar./Apr. 2001.

[25] L. Maharjan, T. Yoshii, S. Inoue, and H. Akagi, "A transformerless energy storage system based on a cascade PWM converter with star configuration," *IEEE Trans. Ind. Appl.*, vol. 44, no. 5, pp. 1621–1630, Sep./Oct. 2008.

Laxman Maharjan (S'06–M'10) was born in Lalitpur, Nepal, on January 2, 1979. He received the B.E. degree in electrical engineering from Institute of Engineering, Tribhuvan University, Lalitpur, Nepal, in 2002, and the M.S. and Ph.D. degrees in electrical and electronic engineering from Tokyo Institute of Technology, Tokyo, Japan, in 2007 and 2010, respectively.

From October 2004 to March 2005, he was a Research Student in Tokyo Institute of Technology. Since 2010, he has been with Fuji Electric Company Ltd. His current research interests include multilevel cascade converters and energy storage systems.

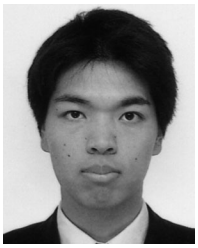

Tsukasa Yamagishi was born on June 15, 1985. He received the B.S. and M.S. degrees in electrical and electronic engineering from Tokyo Institute of Technology, Tokyo, Japan, in 2008 and 2010, respectively.

Since 2010, he has been with Mitsubishi Heavy Industries Ltd. His current research interests include multilevel cascade converters.

Hirofumi Akagi (M'87–SM'94–F'96) was born in Okayama, Japan, in 1951. He received the B.S. degree from the Nagoya Institute of Technology, Nagoya, Japan, in 1974, and the M.S. and Ph.D. degrees from the Tokyo Institute of Technology, Tokyo, Japan, in 1976 and 1979, respectively, all in electrical engineering.

In 1979, he joined the Nagaoka University of Technology, Nagaoka, Japan, as an Assistant Professor and then Associate Professor in the Department of Electrical Engineering. In 1987, he was a Visiting Scientist at the Massachusetts Institute of Technology (MIT), Cambridge, for ten months. From 1991 to 1999, he was a Professor in the Department of Electrical Engineering, Okayama University, Okayama, Japan. From March to August of 1996, he was a Visiting Professor at the University of Wisconsin, Madison, and then MIT. Since January 2000, he has been a Professor in the Department of Electrical and Electronic Engineering at the Tokyo Institute of Technology. He is the author or coauthor more than 100 IEEE Transactions papers and two invited papers published in *Proceedings of the IEEE* in 2001 and 2004. The total citation index for all his papers in *Google Scholar* is more than 15 000. He has made presentations many times as a keynote or invited speaker internationally. His current research interests include power conversion systems, motor drives, active and passive EMI filters, high-frequency resonant inverters for induction heating and corona discharge treatment processes, and utility applications of power electronics such as active filters, self-commutated back-to-back systems, and flexible ac transmission systems devices.

Prof. Akagi served as the President of the IEEE Power Electronics Society from 2007 to 2008, and is currently the Senior Past President. He was elected as a Distinguished Lecturer of the IEEE Power Electronics and Industry Applications Societies during 1998–1999. He was the recipient of the five IEEE Transactions Prize Paper Awards and nine IEEE Conference Prize Paper Awards, the 2001 IEEE William E. Newell Power Electronics Award, the 2004 IEEE Industry Applications Society Outstanding Achievement Award, and the 2008 IEEE Richard H. Kaufmann Technical Field Award.